Research Journal of Pharmaceutical, Biological and Chemical Sciences

Modeling The Reactions of Converting Heteroatom-Containing Components of Heavy Oil Fractions During Hydroconversion.

Khusain Magamedovich Kadiev[1,2]*, Agadjan Mirza Gyul'maliev[2],
Natalia Vladimirovna Oknina[1] ,Alexander Evgenievich Batov[1,2],
Malkan Khusainovna Kadieva[1,2], and Askhab Umaltovich Dandaev[1,2].

[1]Public Joint-Stock Company "Elektrogorsk Institute of Oil Refining" Budenova street 5, Elektrogorsk, 142530 Russia.
[2]Topchiev Institute of Petrochemical Synthesis, Russian Academy of Sciences pr. Leninskii 29, Moscow, 119991 Russia.

ABSTRACT

The article gives the results of studying the efficiency of heteroatom compounds removal from the heavy residue of the oil sludge organic part in the conditions of catalytic hydroconversion. The results of determining the elemental and group hydrocarbon composition of the initial 520°C+ residue of the reservoir oil sludge organic part and 520°C+ fraction obtained from hydroconversion products have shown high conversion of paraffin-naphthene hydrocarbons, resins and aromatics. By applying the methods of chemical thermodynamics and quantum chemistry, it has been shown that in the conditions of hydroconversion of the heavy residue, O-containing compounds are easier to convert than N- and S-containing ones, and it is much easier to convert model N-containing components than S-containing.

Keywords: oil sludge, reservoir sludge, hydroconversion, heteroatoms, thermodynamic analysis, quantum chemistry, ultradisperse catalyst, molybdenum.

*Corresponding author

INTRODUCTION

Oil sludges are heavy bulk wastes of oil refineries [1-5]. Oil sludges properties are similar to those of oil residues, but they additionally contain a significant amount of emulsion water and mechanical and mineral impurities. This feature of oil sludges complicates efficient separation of the hydrocarbon part and its further refining. High number of asphalt-resinous compounds, metals and sulfur in the hydrocarbon part of heavy oil residues does not allow refining them by using currently existing industrial technologies. For their removal to obtain engine oil, the methods of hydrogenate refining of heavy oil residues can be successfully applied as described in [6], which has been utilized for various types of feed and intended to obtain as much as possible distillate oil products from heavy hydrocarbon feed [7-9]. Heteroatom-containing components of the hydrocarbon part of oil sludges impair many performance characteristics of oil products obtained after their refining, and represent an undesirable burden and reduce the calorific value of fuel fractions. So, the issues of their removal and increasing the quality of sales products are one of the most important in the catalytic hydroconversion of oil sludges [10].

Heteroatom-containing compounds are distributed evenly by fractions [11-12]. Their largest part is concentrated in heavy fractions, mainly in asphalt and resinous components contained in the fractions of higher boiling point. Oxide-containing compounds in oil are represented by oxides, ethers, phenols, etc. Unlike other heteroelements mainly contained in the asphalt and resinous part of oil, sulfur is present in significant amount in distillate fractions [11]. In tars and oil sludges, the content of heteroatoms is higher than in initial oils.

The degree of heteroatoms (S, N and O) removal in the conditions of hydroconversion can depend on several factors: the nature of heteroatoms, structural peculiarities and reaction capability of heavy feed fragments which include heteroatoms in bound form, and the catalyst activity.

The study results of the elemental and structural hydrocarbon composition of 520°C+ residue of the initial oil sludge organic part and residues after its hydroconversion show that these feed properties are similar to those of heavy oil residues. By applying methods of chemical thermodynamics and quantum chemistry, a theoretical analysis of the heteroatom relative degree of removal was performed in the conditions of catalytic hydroconversion.

EXPERIMENTAL

Experiments of hydroconversion of the oil sludge organic part were carried out in the presence of in-situ synthesized nano-size and ultradisperse particles of molybdenum-containing catalyst [13]. As a catalyst precursor, the water-soluble salt of molybdenum-ammonium paramolybdate was used $(NH_4)_6Mo_7O_{24} \cdot 4H_2O$. The catalyst content in the reaction zone on Mo-basis was 0.05 wt%. The precursor was charged with water solution, water content in the reaction zone being 2.0 wt%.

In studies, an organic part of oil sludge was taken as initial feedstock from the tank after its pre-conditioning in accordance with the methodology previously described in [14]. The oil sludge organic part was pre-fractioned and 350°C+ was obtained, that was used as a feed in hydroconversion experiments. To obtain evenly distributed nano-particles of catalyst, the synthesis of MoS_2 active phase from the emulsion was used. The catalyst was sulfided in situ in the reactor during hydroconversion as a result of interaction between precursor destruction products with hydrogen sulphide *[15-16]* formed during the thermal cracking of sulfur containing feed components in the hydrogen atmosphere. The catalyst precursor water solution of specified concentration and amount was injected into the feed (350°C+ fraction) heated to 95°C, and mechanical dispersion was performed by using a rotary cavitation agent disperser intended for mixing and homogenizing of various materials in liquid media, for 30-40 minutes at 15,000 rpm. The temperature in the vessel for initial mixing of components was maintained below 90-95°C to prevent water phase boiling. Hydroconversion experiments were conducted on the hydroconversion unit [13-14].

To assess the conversion degree of highly molecular component, the structural grouped analysis of samples was carried out by using liquid adsorption chromatography with gradient displacement and separation by using Gradient-M laboratory liquid chromatograph. The chromatograph is designed to analyze heavy oil products boiling away at 300°C: bitumen, tar, fuel oil, asphaltenes, cracking residues. The chromatograph

operating principle consists in gradient separation of the analyzed product in the chromatographic column by a mobile phase stream containing a mixture of solvents selected for a specific application, eluent transfer in the form of a film to the transportation chain, eluent removal from the chain in the evaporator, thermal oxidizing destruction of separate components of the analyzed substance in the oxidizing cell in the presence of oxygen, air and copper oxide, and detection of the generated carbon dioxide with a catharometer.

The detector signal record is a chromatogram, with every group corresponding to a specific peak (paraffin-naphthene, light aromatics (monocyclic), medium aromatics (bicyclic), heavy aromatics (polyciclyc), neutral and acid tars, and asphaltenes).

Formation of the solvent gradient in the chromatographic column by using frontal chromatography allows separating high boiling oil products by the number of groups corresponding to the number of solvents, and solvents sufficiently differ in the extent of their interaction with the adsorbent. The qualitative and quantitative composition of groups is defined by adsorbent properties and solvent concentration. To separate the malthene part of the oil product, complex solvent I is used (isooctane, dichloroethane, diisoamyl ether, ethyl acetate, ethyl alcohol), and for asphaltene desorption, solvent II is used (benzene chloride, ethyl alcohol). Asphaltenes are determined within a single chromatographic process, and the second eluent is supplied after desorption from the malthene part column. Benzene and cyclohexane are injected in the mobile phase by means of dissolving 0.1 g of the analyzed sample in the cyclohexane/benzene mixture (1:1) at the ratio of 1:7 at the stage of preparation of analyzed oil products.

To determine the content of carbon, hydrogen, nitrogen, sulfur and oxygen, CHNS-O automatic elemental micro-analyzer Euro EA 3000 was used. Its principle of operation consists in dynamic combustion in a flash with further chromatographic separation of generated gaseous combustion products. Pressurized oxygen injection by using this principle is very well demonstrated by an extremely bright flash in the reactor that can be seen through a special inspection port. This flash guarantees full combustion even of most complicated matrices. The sub-sample contained in a thin-wall tin capsule is placed in the autosampler cell. The sample is discharged to the reactor zone; at the same time, it is supplied with a portion of oxygen cleaned from nitrogen, carbon and moisture. Oxygen is supplied under an optimized injection scheme patented by Eurovector with respect to the type and size of the sample. An exothermic reaction accompanied by the formation of nitrogen and carbon oxides, sulfur, halogens and hydrogen occurs at 1800°C. Along with the inert carrier gas (helium), the mixture of gaseous products goes through the catalyst bed. Further oxidation of nitrogen and carbon oxides occurs on its surface. The mixture thus obtained is cleaned from combustion products and is supplied to the catalyst second bed where nitrogen oxides are reduced to nitrogen. The gas mixture (N_2, CO_2, H_2O and SO_2 in general case) is divided by the embedded chromatographic column. All signals typical of each components of the gas mixture are recorded by the detector by heat conductivity and are processed by Callidus software.

RESULTS

The results of experimental studies of the initial feed and hydroconversion residue are given in Table 1. Additionally, the insaturation degree of residues was calculated according to methodology [17].

Table 1. Properties of feed and hydroconversion residue

Parameter	Feed, 520°C+ fraction	Hydroconversion residue, 520°C+ fraction	Absolute change in content, wt%
Yield, wt%	46.1	13.8	
Grouped hydrocarbon composition, wt%			
Paraffins and napthenes	27.4	4.6	-95
Aromatics	46.1	39.0	-74
Resins	21.3	29.3	-59
Asphaltenes	5.3	27.1	+52
Elemental composition, wt%			
N	0.5	0.4	-23
C	84.0	83.8	
H	10.5	11.0	

	4.6	4.0	-26
S			
O	0.4	0.8	-60
H/C atomic ratio	1.5	1.6	
Structure insaturation degree, δ	3.54	2.99	-

To analyze the results obtained in the article, the methods of chemical thermal dynamics were used. Upon the example of compound imitating S, N and O-containing structural fragments of heavy oil residues, their relative thermal stability was evaluated, along with the reactivity and the extent of heteroatom removal in hydrogenation reaction with all other conditions being the same. The list of model compounds selected for analysis is given in Figure 1 (a-c).

Calculations of thermal dynamic functions: ΔH – heat content, ΔS – entropy and ΔG – Gibbs energy are made for the conditions of ideal gas.

The equilibrium reaction composition was determined from the minimum of Gibbs energy ΔG_{useful} [18-19] using the following equation:

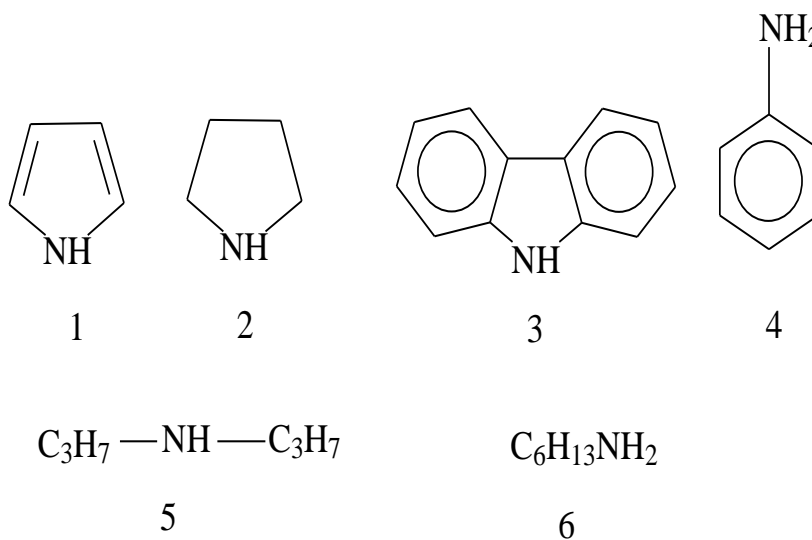$$\Delta G_{useful} = \sum_{i=1}^{M} n_i(\Delta G_i^0 + RTln(P)) + RT \sum_{i=1}^{M} n_i ln n_i - RTnln(n)$$

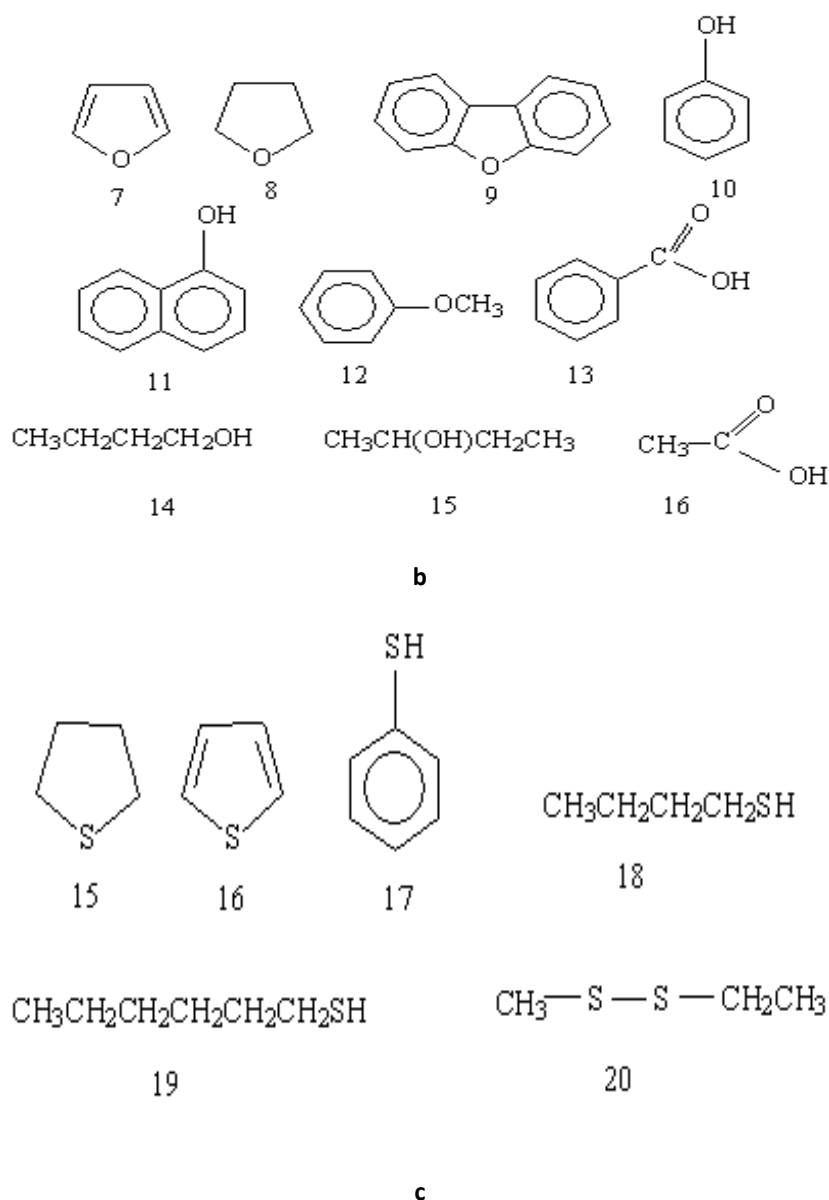with respect to the following equations of material balance:

$$\sum_{i=1}^{M} a_{ji}\, n_i = b_i;\ j = 1,2,\dots,m.$$

$$\sum_{i=1}^{M} n_i - n = 0$$

where ΔG^0 – standard Gibbs energy; n_i – number of moles of i-th component; n – total number of moles in the system; T – absolute temperature, K; P – pressure, MPa; a_{ji} – stoichiometric coefficients of component formation reactions (from atoms); m – number of atom types; b_i – initial number of gram atoms of j-th type of atom in the system; M – total number of components.
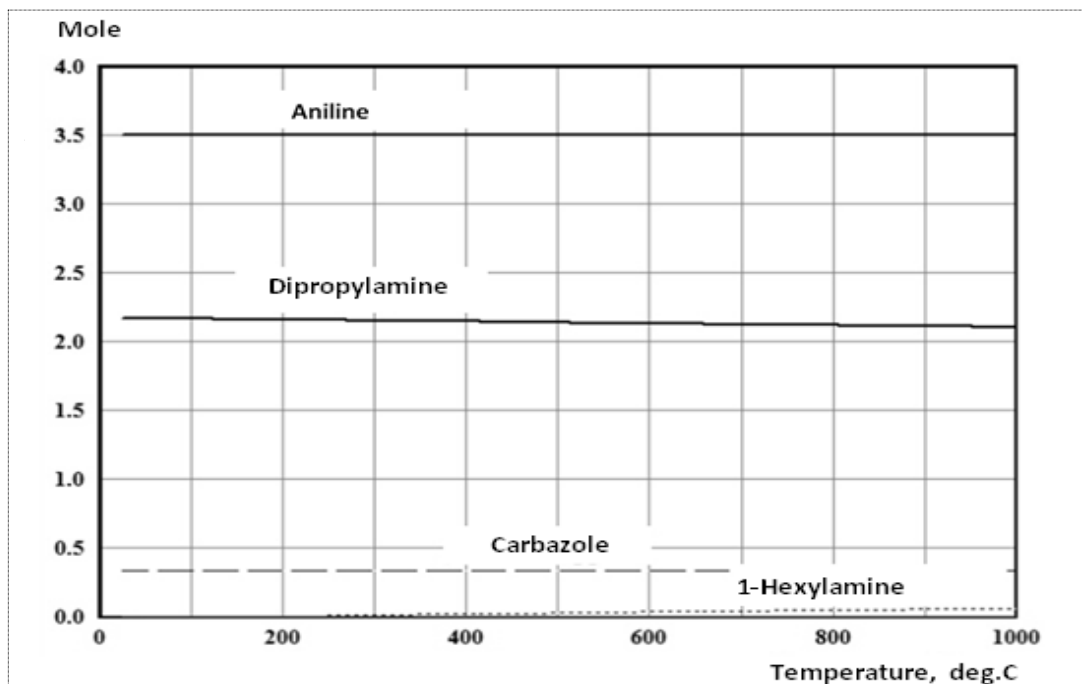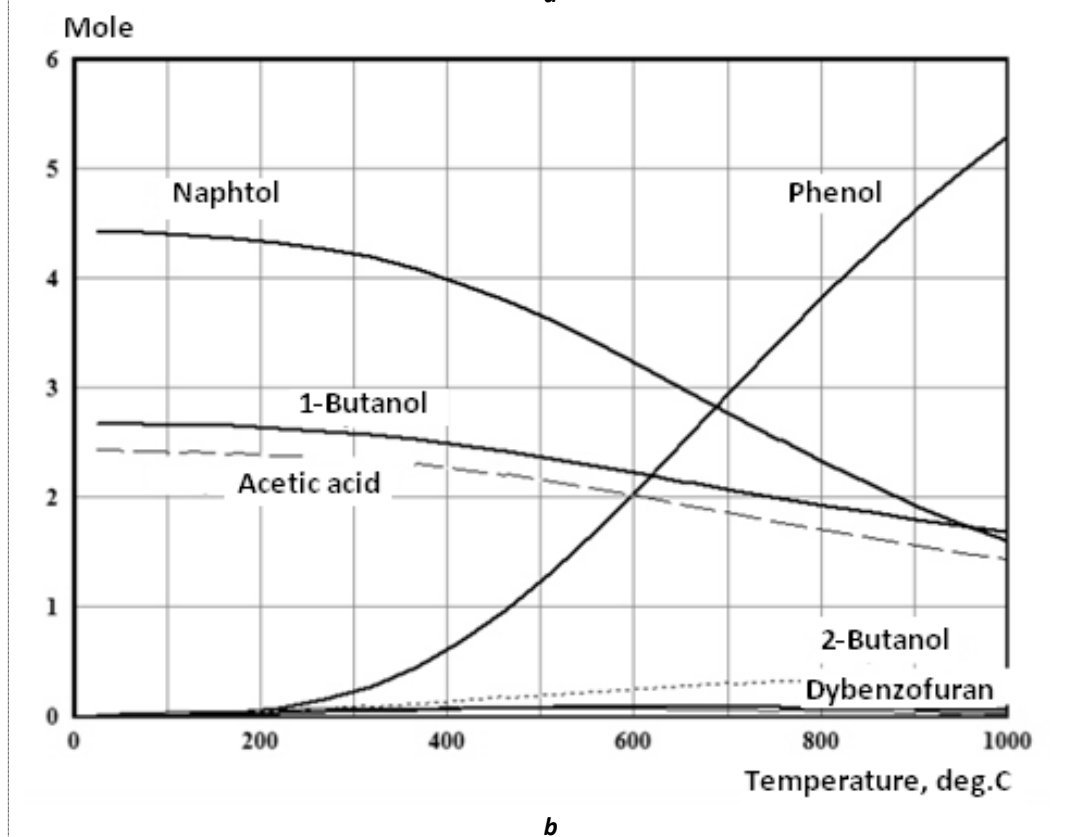

a

Figure 1. Chemical formulas of model compounds: a – N-containing (1-pyrrol, 2-tetrahydropyrrole, 3-carbazole, 4-aniline, 5-dipropylamine, 6-1-hexylamine), b – O-containing (7-furan, 8-tetrahydrofuran, 9-dibenzofuran, 10-phenol, 11-naphthol, 12-benzyl methyl ether, 13-benzoic acid, 14-1-butanol, 15-2-butanol, 16-acetic acid), c – S-containing (15-tetrahydrothiophene, 16-thiophene, 17-thiophenol, 18-butanethiol-1, 19-hexanethiol-1, 20-dithiopentane-2,3).

The relative thermal stability of S, N, and O-containing compounds was assessed upon the results of thermodynamic calculations of the equilibrium composition upon temperature [20]. Calculations were made at P=7 MPa and initial concentrations of each compound of 1 mole. Calculations results for S, N, and O-containing compounds are given in Figure 2 (a-c).
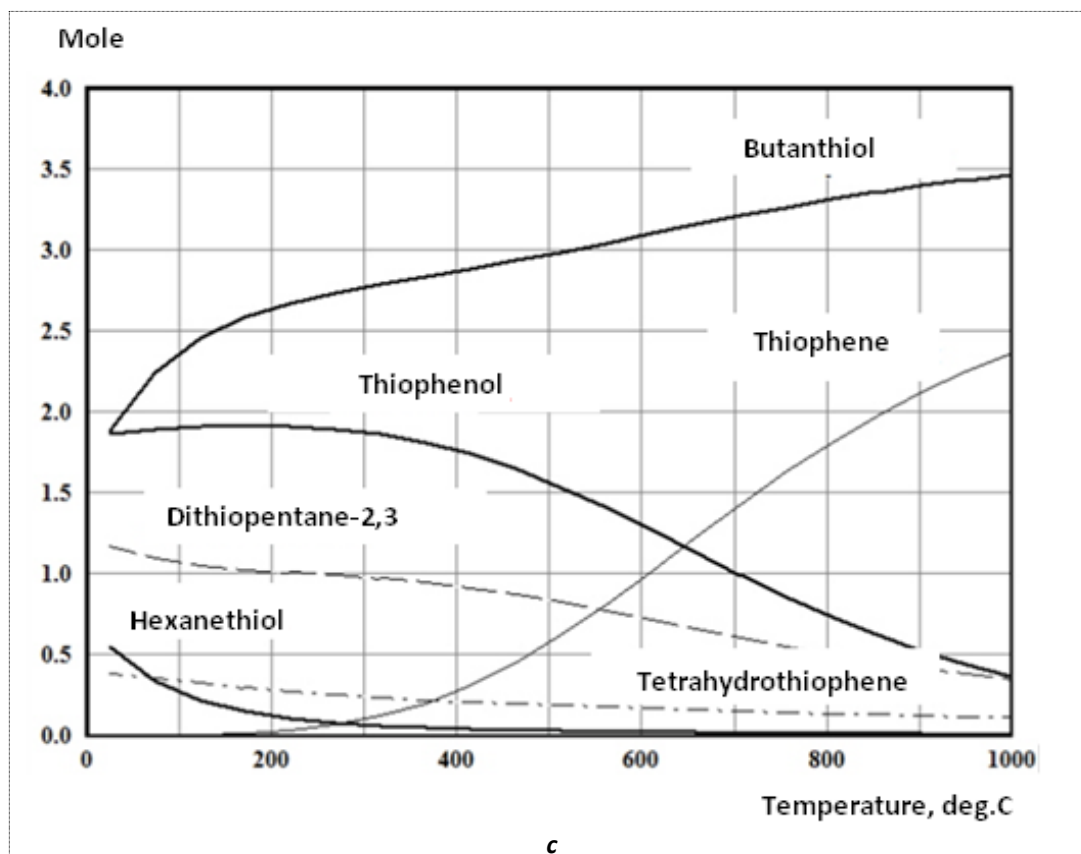
a

b

Figure 2. Temperature dependency of the equilibrium composition of N (*a*), O (*b*) and S-containing (*c*) compounds.

Upon the example of total schemes of model reactions of hydrogenation given in Figure 3 (a, b), the changes of thermal dynamic characteristics of heteroatom removal reactions were considered, and the comparative analysis of their values was performed, which are defined by the nature of heteroatoms $X = -NH-, -O-, -S-$. Temperature dependencies of thermal-dynamic functions ΔH, ΔS and ΔG are given in Tables 2 and 3 for these reactions.
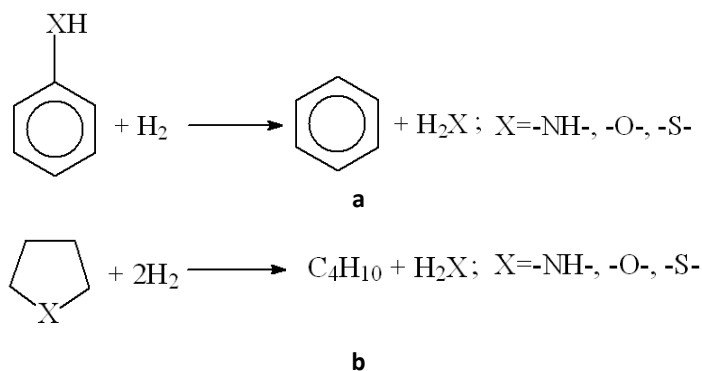

Figure 3. Schemes of model reactions: a – hydrogenation of aromatic heteroatom-containing compounds, b – hydrogenation of naphthenic heteroatom-containing compounds.

According to the equation $\Delta G = \Delta H - T\Delta S$, self-existing reaction in the conditions of $\Delta G < 0$, is possible only on two cases: $\Delta H < 0$, e.g., the reaction is exothermic, and when the value of the thermodynamic functions is $\Delta H > 0$, the reaction is endothermic, but the absolute value is $|T\Delta S| > \Delta H$.

Table 2. Temperature dependency of thermal dynamic functions for reactions a (Figure 3)

T, °C	$C_6H_7N + H_2 = C_6H_6 + NH_3$			$C_6H_6O + H_2 = C_6H_6 + H_2O$			$C_6H_6S + H_2 = C_6H_6 + H_2S$		
	ΔH	ΔS	ΔG	ΔH	ΔS	ΔG	ΔH	ΔS	ΔG
	Kcal/ mole	Cal/ mole·K	Kcal/ mole	Kcal/ mole	Cal/ mole·K	Kcal/ mole	Kcal/ mole	Cal/ mole·K	Kcal/ mole
0	-11/827	3/335	-12/737	-14/855	3/135	-15/711	-11/848	2/136	-12/431
100	-12/255	1/995	-13/000	-15/245	1/919	-15/962	-12/234	0/930	-12/581
200	-12/657	1/040	-13/149	-15/642	0/976	-16/104	-12/586	0/094	-12/630
300	-13/062	0/265	-13/213	-16/022	0/248	-16/164	-12/938	-0/582	-12/605
400	-13/467	-0/387	-13/206	-16/375	-0/321	-16/159	-13/296	-1/157	-12/517
500	-13/856	-0/927	-13/140	-16/700	-0/771	-16/104	-13/649	-1/645	-12/376
600	-14/207	-1/354	-13/025	-16/995	-1/131	-16/008	-13/978	-2/046	-12/191
700	-14/494	-1/666	-12/873	-17/261	-1/419	-15/880	-14/263	-2/356	-11/970
800	-14/727	-1/894	-12/694	-17/497	-1/651	-15/726	-14/483	-2/572	-11/723
900	-14/908	-2/056	-12/496	-17/706	-1/837	-15/551	-14/617	-2/692	-11/459
1,000	-15/042	-2/165	-12/285	-17/888	-1/986	-15/360	-14/643	-2/713	-11/188

Table 3. Temperature dependency of thermal dynamic functions for reactions b (Figure 3)

T, °C	$C_6H_9N + 2H_2 = C_4H_{10} + NH_3$			$C_6H_8O + 2H_2 = C_4H_{10} + H_2O$			$C_6H_8S + 2H_2 = C_4H_{10} + H_2S$		
	ΔH	ΔS	ΔG	ΔH	ΔS	ΔG	ΔH	ΔS	ΔG
	Kcal/ mole	Cal/ mole·K	Kcal/ mole	Kcal/ mole	Cal/ mole·K	Kcal/ mole	Kcal/ mole	Cal/ mole·K	Kcal/ mole
0	-40/269	-16/135	-35/861	-43/932	-14/258	-40/038	-26/893	-12/964	-23/351
100	-40/363	-16/411	-34/239	-43/989	-14/420	-38/609	-27/274	-14/137	-21/998
200	-40/598	-16/964	-32/571	-44/189	-14/890	-37/144	-27/762	-15/296	-20/525
300	-40/905	-17/552	-30/845	-44/439	-15/369	-35/630	-28/246	-16/225	-18/947
400	-41/246	-18/100	-29/062	-44/703	-15/793	-34/072	-28/684	-16/930	-17/288
500	-41/591	-18/578	-27/227	-44/963	-16/153	-32/474	-29/062	-17/454	-15/567
600	-41/915	-18/972	-25/349	-45/211	-16/455	-30/843	-29/378	-17/839	-13/801
700	-42/193	-19/274	-23/436	-45/445	-16/709	-29/185	-29/635	-18/119	-12/003
800	-42/421	-19/498	-21/497	-45/664	-16/923	-27/503	-29/842	-18/321	-10/180
900	-42/553	-19/616	-19/540	-45/868	-17/105	-25/801	-30/009	-18/471	-8/340
1,000	-42/570	-19/631	-17/577	-46/060	-17/262	-24/082	-30/149	-18/585	-6/487

Upon the example of hydrogenation reactions I-VI for sulfur-containing compounds, modeling structural fragments of heavy residue, the schemes of which are given below, a comparative analysis of Gibbs energies has been done, and it has been shown which reactions that occur with hydrogen sulfide removal are most probable. The calculation results are given in Figures 4 and 5 and in Table 4.
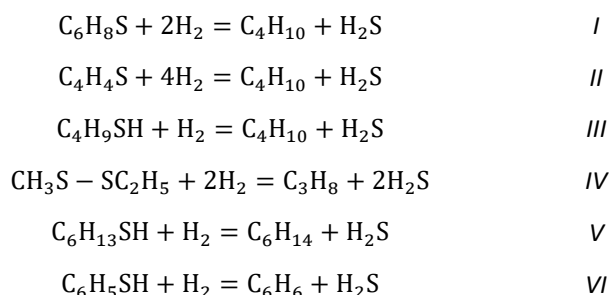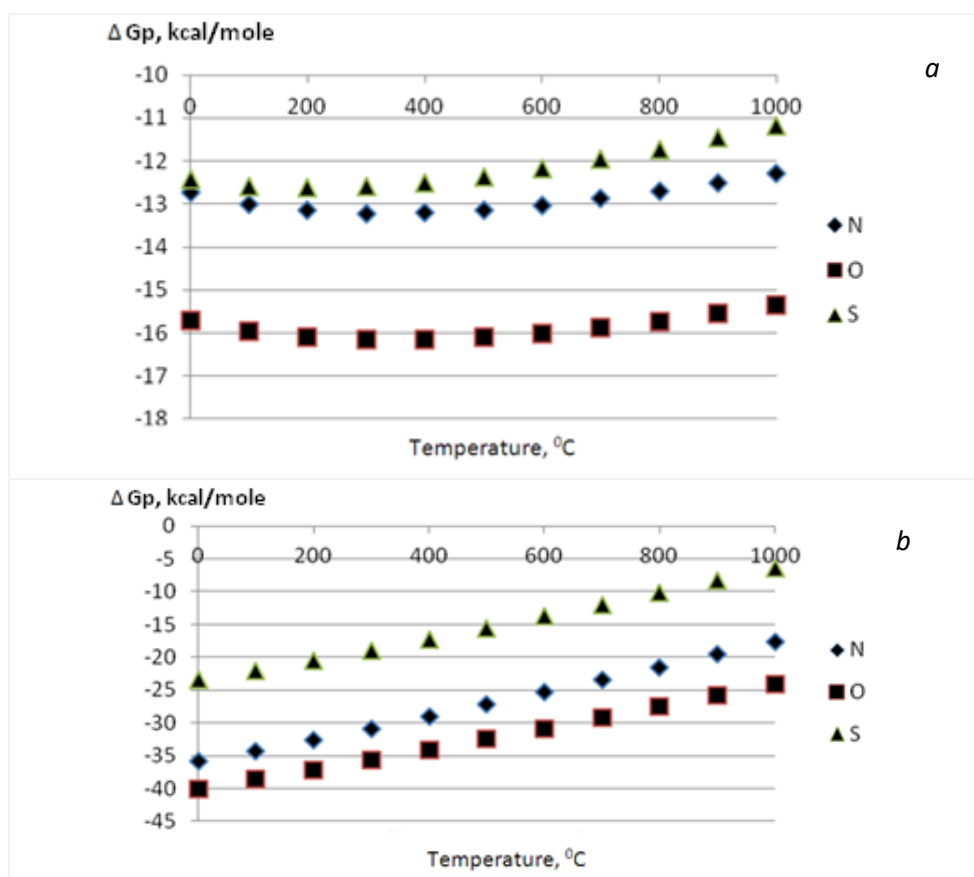
$$C_6H_8S + 2H_2 = C_4H_{10} + H_2S \qquad I$$

$$C_4H_4S + 4H_2 = C_4H_{10} + H_2S \qquad II$$

$$C_4H_9SH + H_2 = C_4H_{10} + H_2S \qquad III$$

$$CH_3S - SC_2H_5 + 2H_2 = C_3H_8 + 2H_2S \qquad IV$$

$$C_6H_{13}SH + H_2 = C_6H_{14} + H_2S \qquad V$$

$$C_6H_5SH + H_2 = C_6H_6 + H_2S \qquad VI$$

Table 4. Temperature dependency of Gibbs energy for reactions (I-VI)

T, °C	ΔGp, Kcal/mole					
	I	II	III	IV	V	VI
0	-23.351	-44.095	-14.607	-25.449	-14.525	-12.431
100	-21.998	-37.179	-14.806	-26.458	-14.726	-12.581
200	-20.525	-29.919	-14.914	-27.369	-14.826	-12.630
300	-18.947	-22.416	-14.94	-28.316	-14.838	-12.605
400	-17.288	-14.744	-14.895	-29.373	-14.777	-12.517
500	-15.567	-6.958	-14.784	-30.585	-14.655	-12.376
600	-13.801	0.904	-14.616	-31.980	-14.486	-12.191
700	-12.003	8.812	-14.396	-33.576	-14.279	-11.970
800	-10.180	16.748	-14.129	-35.382	-14.044	-11.723
900	-8.340	24.696	-13.819	-37.405	-13.79	-11.459
1,000	-6.487	32.646	-13.470	-39.644	-13.524	-11.188

Figure 4. Dependency of Gibbs energy ΔG on temperature: a – for reaction (a, Figure 3), b – for reaction (b, Figure 3).
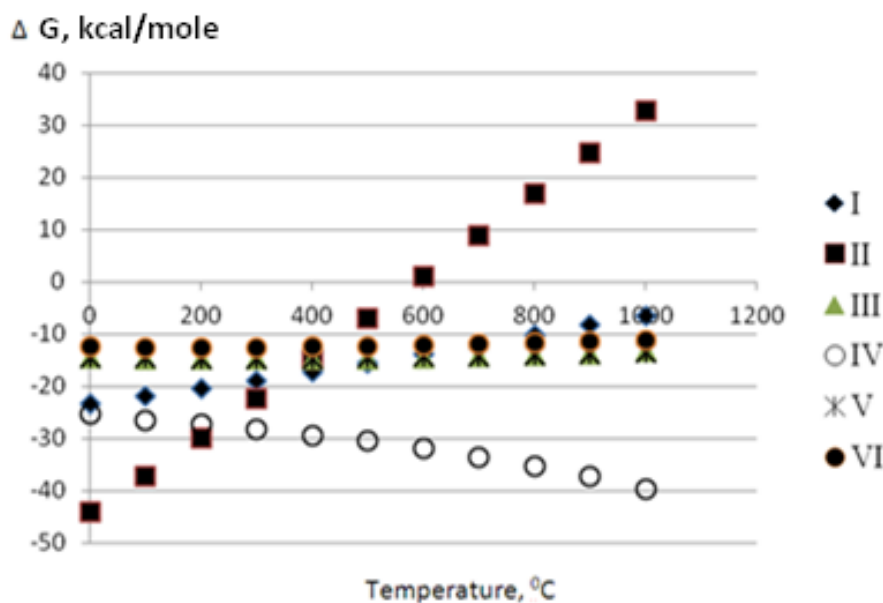
Figure 5. Charts of function ΔG =f(T) for reactions (I-VI).

To evaluate the catalyst role in removal reactions of feed sulfur-containing components during hydro-conversion, the reaction was studied that imitates sulfur removal from most thermodynamically stable sulfur-containing structures. By applying the quantum chemical calculation method for the molecule's electronic structure, the thiophene chemosorption reaction on the molybdenum disulfide cluster was studied. Calculations were made by using the energy from DFT B3LYP/ DGDZVP (5D, 7F) electronic density with full optimization of molecule's geometric parameters and calculation of frequencies of normal oscillations. The results of quantum chemical calculations are demonstrated in Figures 6 and 7 (a-d).

Gibbs energy G for reactions I-III was calculated with respect to electronic energy of components E_{elec}, by using the following formulas [11]:

$$E_0 = E_{elec} + E_{ZPE}$$

$$E = E_0 + E_{vib} + E_{rot} + E_{trans}$$

$$H = E + RT$$

$$G = H - TS$$

Where E_{elec} – electronic energy; E_{ZPE} – energy of zero oscillations; E_{vib} – oscillating energy; E_{rot} – rotation energy; E_{trans} – translation energy of a molecule; R – universal gas constant.

According to the data given in Figure 6, the Hartree-Fox energy of chemosorption (ΔE_{HF}) is:

$$\Delta E_{HF} = E(C_4H_4S \cdots Mo_2S_4) - E(C_4H_4S) - E(Mo_2S_4) = -0.0970761\, a.\,e. = -60.92 \frac{kcal}{mole},$$

and Gibbs energy is:

$$\Delta G = G(C_4H_4S \cdots Mo_2S_4) - G(C_4H_4S) - G(Mo_2S_4) = -0.073673\, a.\,e. = -46.21 \frac{kcal}{mole}$$

E_{HF}=-552.9884131 a.e.
G=-552.949218 a.e.

E_{HF}=-9546.9955056 a.e.
G=-9547.023835 a.e.
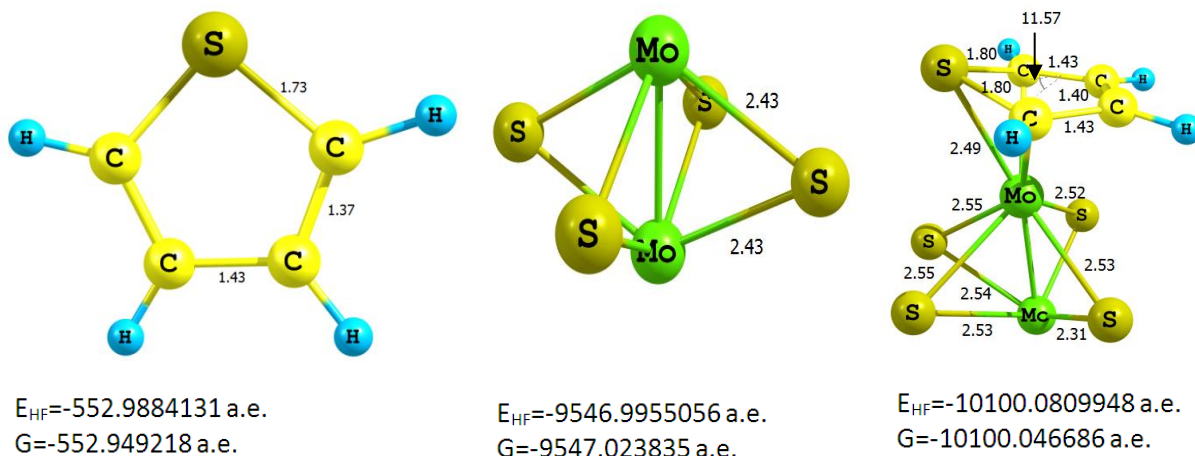
E_{HF}=-10100.0809948 a.e.
G=-10100.046686 a.e.

Figure 6. Calculation results of energetic and geometric characteristics of thiophene C_4H_4S, Mo_2S_4 cluster and $C_4H_4S \cdots Mo_2S_4$ complex.
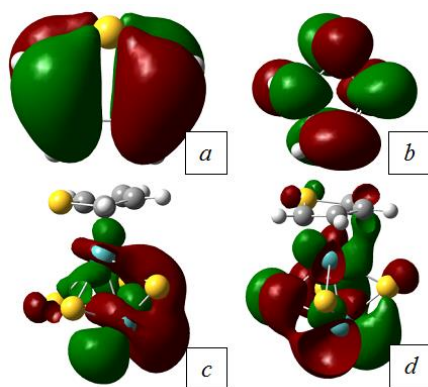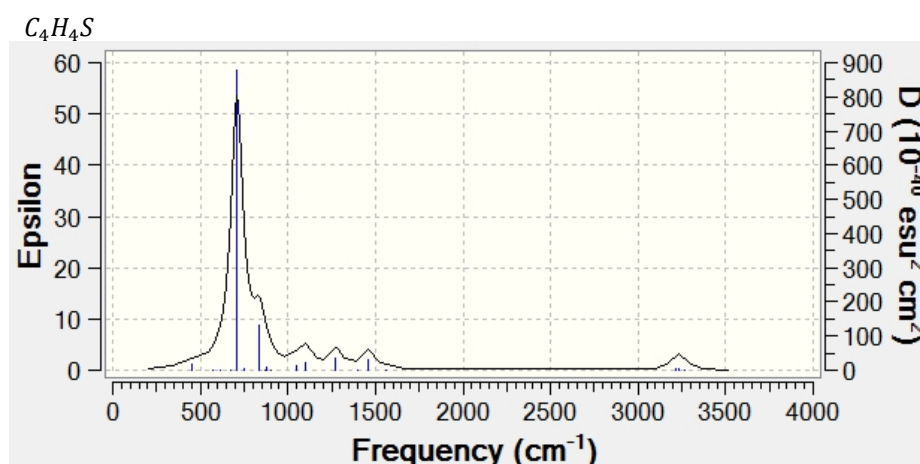

Figure 7. Upper occupied π_g (a) and lower vacant π_u (b) molecular orbitals of thiophene, respectively, (c) and (d) of $C_4H_4S \cdots Mo_2S_4$ complex.

Figure 8 gives IR-spectra of the molecule C_4H_4S, and the complex [$C_4H_4S \cdots Mo_2S_4$], calculated under the quantum chemical method DFT B3LYP/ DGDZVP (5D, 7F), in cm^{-1} THz. Symmetric deformation oscillation frequency of a dihedral angle ∠CCCS is 382 cm^{-1} (11 THz), that for valent linkage C − S 562 cm^{-1} (17 THz).
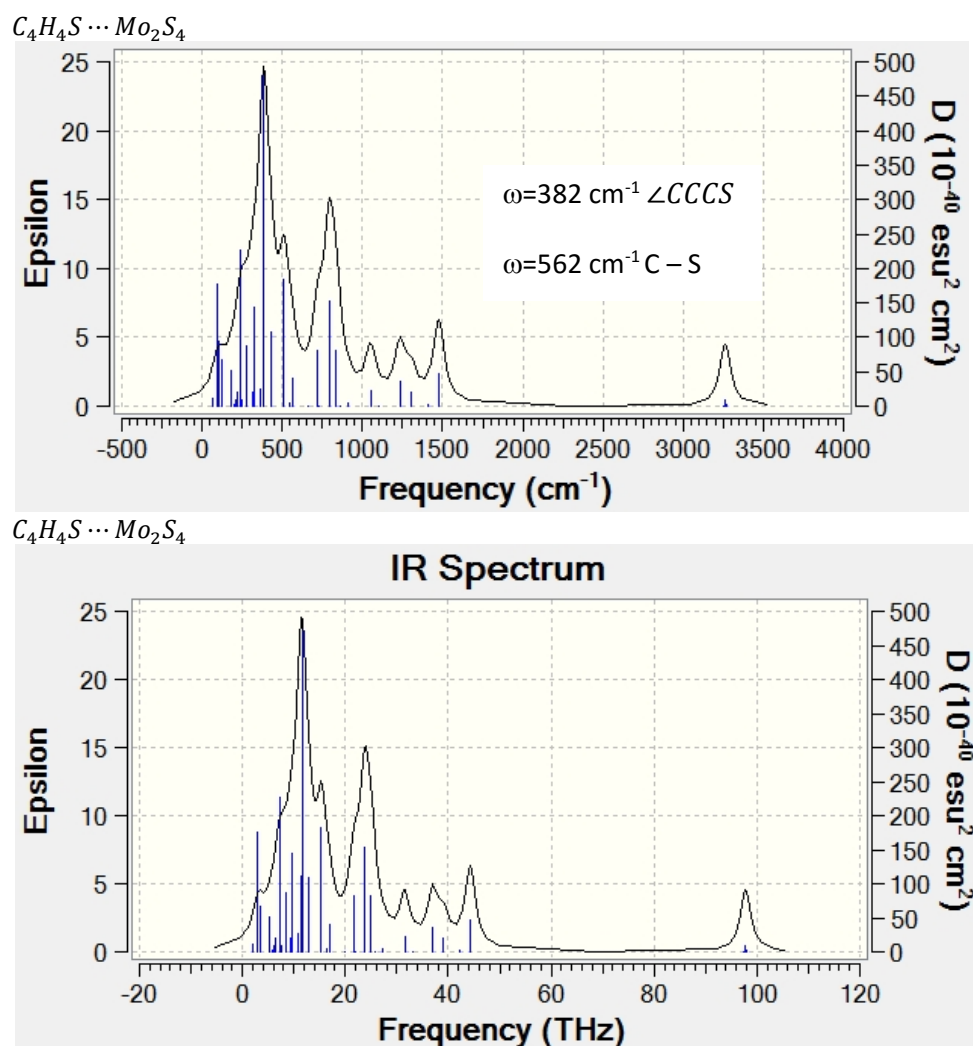
$C_4H_4S \cdots Mo_2S_4$

$C_4H_4S \cdots Mo_2S_4$

Figure 8. IR-spectra for C_4H_4S and complex $C_4H_4S \cdots Mo_2S_4$ calculated by using the quantum chemical method DFT B3LYP/ DGDZVP (5D, 7F).

DISCUSSION

Data given in Table 1 shows that as a result of converting the oil sludge organic part during hydrocon-version, the content of 520°C+ residue in reaction products dropped and equaled 13.8 wt%. Significant chang-es take place in hydrocarbon and elemental composition of 520°C+ heavy residue of hydroconversion products as compared to 520°C+ residue properties of initial feed of the hydroconversion. After hydroconversion, in the 520°C+ residue of hydroconversion products, the absolute content of asphaltenes is increased by 52%, which is related to their concentration as a result of reduced content of 520°C+ fraction and formation of secondary asphaltenes from resins and aromatic components. The absolute decrease of content of paraffins, aromatics and resins in the 520°C+ residue after hydroconversion is 95%, 74% and 59%, respectively, which can be relat-ed to predominant destruction of less condensed and more reactive paraffin-naphthenic and aromatic com-pounds.

Table 1 also gives values of insaturation of residues calculated by their elemental composition in ac-cordance with methodology [17]. The structure of compound within the 520°C+ residue after hydroconversion, as seen from the structural parameter value δ (2.99) and H/C ratio (1.6) is more saturated, apparently, because its composition contains more naphthenic structure as compared to the structure of compounds of the initial feed, where δ=3.54.

The comparison of the elemental composition of 520°C+ residues (Table1) shows that for the total conversion level of 70% achieved in hydroconversion, the absolute content of each heteroatom of S, N and O

in the residue reduced: the nitrogen content decreased by 23%, the sulfur content by 26% and the oxygen content by 60%.

In [6], it has been shown that the degree of heteroatom (S, N, O) conversion depending on the reaction time during hydroconversion increases at various rate. To prove this observation, the methods of thermodynamic and quantum chemical analysis were applied to conversion reactions of model components. In particular, it can be seen by the equilibrium composition of model systems depending on the temperature (0-1000K) given in Figure 2a, that among the N-containing compounds under consideration, the most stable are aniline, with dipropylamine being the second in thermal stability. The carbazole and 1-hexylamine concentration is insignificantly small, and the lower stability is shown by pyrrol and tetrahydropyrrole that are fully converted and are absent in equilibrium conditions.

The stability of O-containing compounds strongly depends on the temperature: for low reaction temperatures, the most stable is naphthol, whereas phenol is most stable for high temperatures. According to the data given in Figure 2, the most stable among S-containing compounds are butanethiol, thiophenol and thiofuran. However, according to literature data, the content of thiophene structures in oil is significantly higher than analogs of butanethiol and thiophenol [11].

The analysis of temperature impact upon thermodynamic functions of the studied elemental reactions (Table 2 and 3) has shown that within the entire temperature interval, the hydrogenation reactions under consideration are exothermic ($\Delta H < 0$) and described by negative Gibbs energy values ΔG. Figure 4 gives dependencies ΔG_p on the temperature for schemes of model reactions, which means that heteroatoms have the following thermodynamic probability of removal with all other similar conditions: O > N > S. These conclusions correlate with the results of experimental and calculation data.

The Gibbs energy dependencies on temperature calculated under [20] for reactions (I-VI) (data given in Table 4 and Figure 5) show that the less reactive S-containing compounds in the study conditions are thiophene structures (reaction II). As seen from Figure 6, thiophene is subject to chemosorption on molybdenum atom in cluster Mo_2S_4. In this case, geometric parameters of the thiophene molecules substantially change, just as the between-atom distances in cluster Mo_2S_4. It is evident that the energetic condition of atoms in the studied complex change. For example, the dihedral angle of thiophene $\angle CCCS = 0°$ is increased after chemosorption and becomes ~12°. High energy value of chemosorption (~60.92 Kcal/mole), as well the changes of geometric parameters and the nature of boundary molecular orbitals (Figure 7) indicate that after chemosorption, thiophene is metastable and should easily hydrate and be subjected to destruction with sulfur removal (H$_2$S).

Figure 8 gives IR-spectra of the molecule C_4H_4S, and the complex $C_4H_4S \cdots Mo_2S_4$, calculated under the quantum chemical method DFT B3LYP/ DGDZVP (5D, 7F),in cm^{-1} THz. The values of C-S oscillation frequencies are required if ultrasound impact is used in order to resonantly intensify the sulfur removal reaction. As shown in Figure 8, symmetric deformation oscillation frequency of a dihedral angle $\angle CCCS$ is 382 cm^{-1} (11 THz), that for valent linkage C – S 562 cm^{-1} (17 THz).

The thermodynamic studies show that in the conditions of hydroconversion of the heavy residue, O-containing compounds are easier to convert than N- and S-containing ones, and it is much easier to convert model N-containing components than S-containing. Thermodynamically most stable model fragment of the structure in the heavy residue is the thiophene structure. The quantum chemical calculation of chemosorption energy on the Mo_2S_4 cluster of sulfide molybdenum catalyst experimentally shows that sulfur is coordinated on the molybdenum atom, and the geometry of the Mo sulfide cluster and thiophene changes. This results in increased reactivity of the thiophene ring leading to hydrogenation and sulfur destructive removal.

ACKNOWLEDGMENTS

REFERENCES

[1] Ulitskiy, V.A., Vasil'vitskiy, A.E., & Plushchevskiy, M.B. (2006). *Promyshlennye otkhody i resursosbere-zhenie* [Industrial Waste and Resource Conservation]. Moscow: Sashko.

[2] Shperber, E.R. (2011). Nekotorye vidy otkhodov neftepererabatyvayushchikh zavodov i ikh klassi-fikatsiya [Some Types of Wastes of Oil Refineries and Their Classification]. *Zashchita okruzhayushchey sredy v neftegazovom komplekse, 2*, 27-32.

[3] Hu, G., Li, J., & Zeng, G. (2013). Recent Development in the Treatment of Oily Sludge from Petroleum Industry: A Review. *Journal of Hazardous Materials, 261*, 470-490.

[4] Elektorowicz, M., & Habibi, S. (2005). Sustainable Waste Management: Recovery of Fuels from Petroleum Sludge. *Can. J. Civil. Eng., 32*, 164-169.

[5] Gron' V. A., Korostovenko V. V., Shakhrai S. G.,et al. Problem of generation, reprocessing and disposal of oil sludges. Advances of modern natural science. 2013; 9: 159-162.

[6] Kadiev, Kh.M., Oknina, N.V., Gyul'maliev, A.M., Gagarin, S.G., Kadieva, M.Kh., Batov, A.E., & Khadzhiev, S.N. (2015). K voprosu o mekhanizme i zakonomernostyakh gidrokonversii organicheskoy massy nefteshlamov v prisutstvii nanorazmernykh katalizatorov [On the Mechanism and Main Features of Hydroconversion of the Organic Matter of Oil Sludge in the Presence of Nanosized Catalysts]. *Neftekhimiya, 55(5)*, 418-425.

[7] Khadzhiev, S.N. (2009). Sovremennye tekhnologii glubokoy kompleksnoy pererabotki uglevodorodnogo syr'ya [Modern Technology of Deep Complex Processing of Hydrocarbon Raw Materials]. In *III Rossiyskaya konferentsiya "Aktual'nye problemy neftekhimii"* [III Russian Conference "Actual Problems of Petrochemicals"]. Moscow (Zvenigorod).

[8] Khadzhiev, S. (2008). Proryvnye tekhnologii v sisteme RAN [Groundbreaking Technologies in the System of the Russian Academy of Sciences]. *Khimicheskiy zhurnal, 7-8*, 36-39.

[9] Khadzhiev, S., & Kadiev, K. (2009). Budushchee glubokoy pererabotki nefti: sdelano v Rossii [The Future of Advanced Oil Refining: Made in Russia]. *Khimicheskiy zhurnal, 9*, 34-37.

[10] Kadiev, Kh.M., Gyul'maliev, A.M., Batov, A.E., Kadieva, M.Kh., Oknina, N.V., & Dandaev, A.U. (2015). Strukturnye kharakteristiki rezervuarnogo shlama [Structural Characteristics of Reservoir Sludge]. *Koks i khimiya, 58(11)*, 448-460.

[11] Safieva, R.Z. (1998). *Fizikokhimiya nefti. Fiziko-khimicheskie osnovy tekhnologii pererabotki nefti* [Physical Chemistry of Oil. Physical and Chemical Bases of Technology of Oil Refining]. Moscow: Khimiya.

[12] *Serosoderzhashchie soedineniya* [Sulfur-Containing Compounds]. (n.d.). Retrieved July 6, 2016, from http://www.studfiles.ru/preview/4246981/page:5/.

[13] Khadzhiev, S.N., Kadiev, Kh.M., & Kadieva, M.Kh. (2014). Sintez i svoystva nanorazmernykh sistem - effektivnykh katalizatorov gidrokonversii tyazhelogo neftyanogo syr''ya [Synthesis and Properties of Na-nosized Systems as Efficient Catalysts for Hydroconversion of Heavy Petroleum Feedstock]. *Neftekhimiya, 54(5)*, 323-346.

[14] Oknina, N.V., Kadiev, Kh.M., Maksimov, A.L., Batov, A.E., Kadieva, M.Kh., & Dandaev, A.U. (2015). Studies on Preprocessing of Reservoir Oil Sludges for Further Hydroconversion. *Biosciences Biotechnology Research Asia, 12(Spl. Edn. 2)*, 473-483.

[15] Hanafi, Z.M., Khilla, M.A., & Askar, M.H. (1981). The Thermal Decomposition of Ammonium Heptamolyb-date. *Thermochimica Acta, 45(3)*, 221-232.

[16] Chukin, D., & Nefedov, B.K. (2009). Mekhanizmy sul'fidirovaniya alyumonikel'molibdenovogo katalizatora i ego aktivnost' v reaktsii gidroobesserivaniya tiofena [Mechanisms of Sulphidizing the Aluminium-Nickel-Molybdenum Catalyst and Its Activity in the Reaction of Thiophene Hydrodesulfurization]. *Khimiya tverdogo topliva, 43(6)*, 400.

[17] Kadiev, Kh.M., Gyul'maliev, A.M., Khadzhiev, S.N., & Kadieva, M.Kh. (2010). Primenenie strukturnogo parametra dlya prognoza svoystv vysokomolekulyarnykh organicheskikh soedineniy [Use of the Structure Parameter for Predicting the Properties of High-Molecular-Mass Organic Compounds]. *Neftekhimiya, 50(6)*, 468-471.

[18] Stepanov, N.F., Erlykina, M.E., & Filippov, G.G. (1976). *Metody lineynoy algebry v fizicheskoy khimii* [Methods of Linear Algebra in Physical Chemistry]. Moscow: Moscow State University.

[19] Gyul'maliev, A.M. , Golovin, G.S., & Gladun, T.G. (2003). *Teoreticheskie osnovy khimii uglya* [Theoretical Foundations of Coal Chemistry]. Moscow: Moscow State Mining University.

[20] *HSC Chemistry 6*. (n.d.). Retrieved July 6, 2016, from http://www.hsc-chemistry.net/.